Citation Information:
32nd Aachen Colloquium Sustainable Mobility 2023. Aachen, October 09th to 11th, 2023.
Aachen: Aachener Kolloquium Fahrzeug- und Motorentechnik GbR. Paper No. 094.
ISBN: 978-3-00-076758-6.

Automated and Virtual Optimization of Race-track Simulation Parameters on the Powertrain Test Bench

Jannes **Schilling**; Jan-Michael **Wilmsen** geb. Veith
Department of Verification and Validation, Dr.-Ing. h. c. F. Porsche AG, Stuttgart, Germany

Hans-Christian **Reuss**
Institute of Automobile Engineering, Universität Stuttgart, Stuttgart, Germany

Henrik **Schmidt**; Günther **Prokop**
Chair of Automobile Engineering, Technische Universität Dresden, Dresden, Germany

Contact: jannes.schilling2@porsche.com

Abstract

This paper focuses on powertrain test benches (PTB) in motorsports applications. In this case, a real powertrain is coupled with a virtual environment on the PTB to emulate mechanical loads experienced during racetrack driving. We utilize a Digital Twin of the PTB (a combination of the PTBs' virtual environment, a powertrain model and a testbed model) to reduce setup time and allow offline virtual environment parameterization.

The simulation models of the virtual environment may not always provide accurate representations due to unknown parameters or simplifications made to meet real-time requirements. Consequently, there are discrepancies between PTB and vehicle measurements. This paper aims to minimize such differences with a novel parameter optimization method.

Content

1 Introduction

The competition that has evolved in the automotive industry in recent years requires manufacturers to bring attractive products and innovations to market as early as possible [1]**.** Besides, the primary differentiating feature of vehicles is now no longer hardware components but rather software. The increasing complexity and quantity of software functions have led to a greater demand for testing efforts. Therefore, virtual and partially virtual test methods are integrated into new development processes. [2]

A powertrain test bench serves as a versatile platform for testing the vehicle's lateral and longitudinal dynamics. The test bench generates comparable results to the prototype vehicle in this domain through partially virtual tests. Real-time systems are used to simulate non-existing systems such as environment, residual vehicle and driver. The tests can thus be carried out cost-effectively, reproducibly and at earlier stages.

However, as simulation demands increase, so does the effort needed for model development and parameterization. To ensure realistic results, it is advisable to compare vehicle measurements with test bench measurements and adjust model parameters accordingly. Yet, this method is not feasible for real test benches due to its time-consuming character and potential risk of damaging the Unit Under Test (UUT) during optimization. Therefore, the virtual powertrain test bench already presented by the authors in [3] is suitable for carrying out the process. In this paper, chapter 2 deals with the simulation of the test bench components in more detail. Subsequently, semi-virtual testing and the Digital Twin are presented. The comparison of test bench and vehicle measurements with the subsequent optimization process of the real-time models is presented in chapter 4. Finally, chapter 5 shows further research approaches.

2 The Impact of a Powertrain Test Bench on a Hardware-in-the-Loop Application

A typical Hardware-in-the-Loop (HIL) powertrain test bench setup is illustrated in Fig. 1. The test bench comprises the specimen, test bench-specific components and a device for real-time simulation. We investigate a HIL setup with an electrified powertrain (Electric Drive Unit (EDU)). Here, a battery simulation provides voltage supply and control. The EDU consists of an electric motor, an inverter, and a transmission with included differential and side shafts.

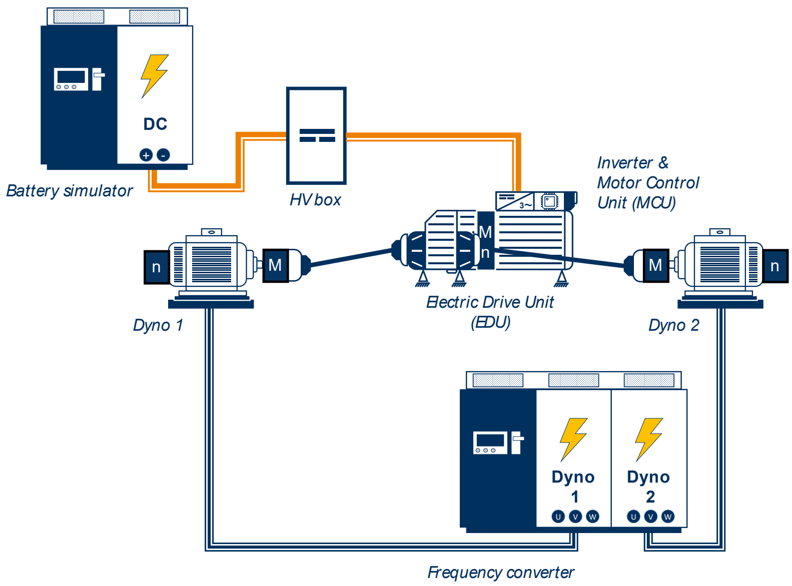

Fig. 1 Powertrain test bench setup: Electric Drive Unit with battery simulation and residual vehicle simulation (HIL)

With the implementation of the EDU into the actual test bench, many interfaces are established. They can be classified into mechanical, electrical or signal transfer domains. For instance, the mechanical assembly of the EDU requires adequate adapters for support and linkage to the dynamometer’s drive side. Moreover, electrical connection is realized by using high-voltage cables to unite the EDU with the battery simulation. And finally, especially in the presence of HIL applications, a signal transfer occurs between the test bench and the residual control loop. In addition, the signal transfer appears between the measurement equipment and the controller. In Fig. 1, the torque transducers (M) are mounted at the drive side of the dynamometer, whereas the angular speed sensors (n) are installed at the opposite back end of the rotor shaft.

In the following section, we will discuss differences in the experimental setup of the same EDU specimen at a test bench compared to a situation where it is assembled inside a reference vehicle. The mechanical and signal transfer domains are essential in motorsports and driving dynamics and hence focused.

2.1 System Performance in the Mechanical Domain

At a powertrain test bench, we substitute the tire-road-interaction with a performant dynamometer, adapters, inline torque transducers and angular speed sensors. Those components can amount to a deviation in mechanical parameters like rotational inertia, torsional stiffness and damping ratio. A powertrain test bench setup can be credited with a deviating torsional stiffness than the reference vehicle. If the test bench influences the system parameters substantially, the system dynamics are changed significantly. We consider a system according to [4] (Eq. 1):

$$\underline{M}\ddot{\vec{q}} + \underline{B}\dot{\vec{q}} + \underline{C}\vec{q} = \vec{0} \qquad \text{Eq. 1}$$

Here, $\underline{M}$, $\underline{B}$ and $\underline{C}$ are the mass, damping and stiffness matrix, and $\vec{q}$ refers to the vector of generalized coordinates, which is, in the present case, mostly a vector of generalized rotational angles. First, an undamped system is considered. For this, the resulting eigenfrequencies are obtained by the specific eigenvalue problem in Eq. 2 incorporating the identity matrix $\underline{E}$ [4]:

$$\left(\underline{M}^{-1}\underline{C} - \vec{\omega}^2\underline{E}\right)\vec{v} = \vec{0} \qquad \text{Eq. 2}$$

Solving leads to the n eigenfrequencies ω_{0i} of the undamped system in Eq. 3 [1, p. 397]:

$$\omega_{0i} = \sqrt{\frac{\gamma_i}{\mu_i}} = \sqrt{\frac{{v_i}^T\underline{C}v_i}{{v_i}^T\underline{M}v_i}}, \quad i = 1,2,\dots,n \qquad \text{Eq. 3}$$

The eigenvector v provides much information about the system modal modes. Especially for comparison of the mechanical parameters of a test bench setup with a vehicle, v allows estimation of the sensitivity of certain parameters under the corresponding natural mode. μ_i represents the modal masses and γ_i reflects the modal stiffnesses of the system for each of the n eigenmodes in Eq. 4 and Eq. 5) [4].

$$\mu_i = \sum_{k=1}^{n} J_k v_{ki}^2, \quad i = 1,2,\dots,n \qquad \text{Eq. 4}$$

$$\gamma_i = \sum_{k=0}^{n} c_{Tk} \left(v_{ki} - v_{k+1,i}\right)^2, \ \ i = 1,2,\dots,n \qquad \text{Eq. 5}$$

In this context, J_k refers to the rotational inertia of the k-th component, whereas c_{Tk} means the torsional stiffness of the same. Finally, the modal sensitivity coefficients for mass μ_{ik} and stiffness γ_{ik} are (Eq. 6 and Eq. 7) [4]:

$$\mu_{ik} = \frac{J_k v_{ki}^2}{\mu_i}, \ \ i = 1,2,\dots,n \qquad \text{Eq. 6}$$

$$\gamma_{ik} = \frac{c_{Tk} \left(v_{ki} - v_{k+1,i}\right)^2}{\gamma_i}, \ \ i = 1,2,\dots,n \qquad \text{Eq. 7}$$

If we assume modal-damped free vibrations, the eigenfrequency ω_i of a damped system is stated with [4] (Eq. 8):

$$\omega_i = \omega_{0i}\sqrt{1 - D_i^2}, \ \ i = 1,2,\dots,n \qquad \text{Eq. 8}$$

In conclusion: If the mechanical system parameters of a specimen at the test bench differ from the system setup of the reference vehicle, one can precisely evaluate the impact on system dynamics. Objective criteria to indicate the test bench impact are the modal sensitivity coefficients. By taking the latter into account, the sensitivity of each component of the test bench setup is derived for each modal mode. Consequently, a simulation-model-based approach can achieve compensation for such an impact of the test bench. If the system performance matters in a particular torsional powertrain mode, respectively frequency range, the dynamometers emulate a compensation torque, for instance. Compensation methods for this field of application are often referred to as *frequency matching* or *road matching* [5],[6].

2.2 System Performance in the Time Dynamics Domain

In addition to the system's mechanical properties, there is an influence of the real-time control loop on system dynamics. Various time delays occur by simulation of the residual vehicle, the environment, and the driver. On one side, the time delays are caused by the computational demand for solving the simulation model's equations at a predefined macro simulation step size. Conversely, time delays arise in signal transfer inside a real-time device and between multiple devices, the test bench controller, actuators, and sensors. For such a system, parameters like *latency*, *dead time*, *jitter,* and *cycle time* determine the fundamental time characteristic [10]. *Latency* refers to a time delay between a system component's input and output value, whereas *dead time* means the initial time delay of a signal at the system's output. The term *jitter* implies a fluctuation in the signal response determined by the difference between maximum and minimum response time [4, p. 316]. Finally, the *cycle time* covers the period from one signal input or request to the next in a cycle-based control system. The concept of cycle times applies to a powertrain test bench, especially to the network or fieldbus interfaces like Ethernet, EtherCAT or CAN-bus. The prefix macro or micro distinguishes the main control process cycle times from the underlying micro tasks. For typical real-time control applications in the powertrain domain, macrocycle times of 1 kHz up to 10 kHz are typical.

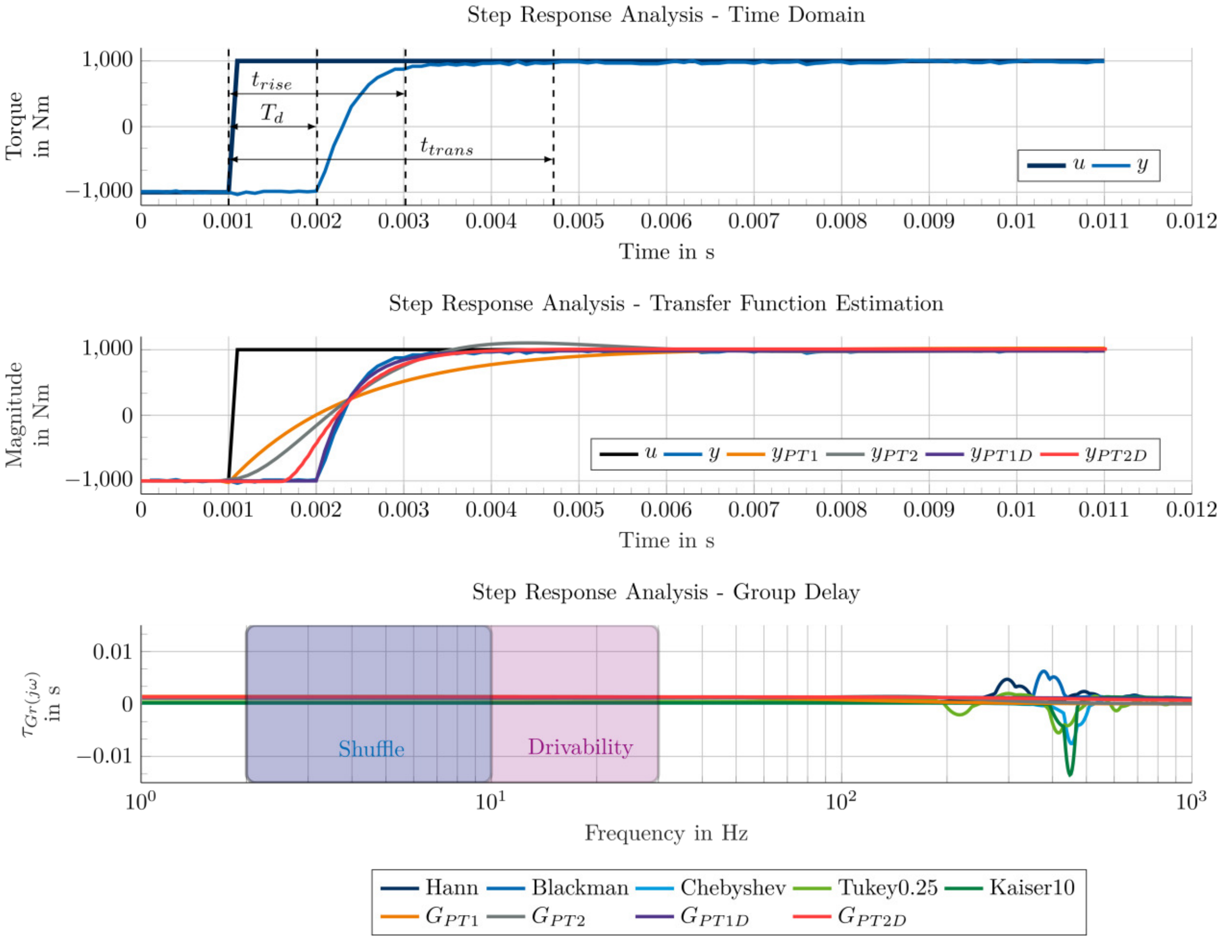

Fig. 2 System identification of the present powertrain test bench's load dynamometers in the time and frequency domain

Unlike a road test, signal transfer and time delay are to be incorporated in a scenario with a test bench and residual vehicle simulation. In that way, the actuator response delay and the complete control loop stability are analyzed. The dominant actuator type at a powertrain test bench is the dynamometer. We use test functions like a step input, sine-sweep input, or white noise to identify the complete control loop. The system response reveals the system dynamics characteristic in the time and frequency domain. In the time domain, a step input's rise time and transient time let to calculate the time delay T_d , rise time t_{rise} and transient time t_{trans}, as presented in-depth in [8]. An experimental analysis of the present powertrain test bench is shown in Fig. 2. While considering a torque-controlled dynamometer in a closed loop at the test bench, T_d refers to the sum of all delays in the overall system (signal transfer, processing time). In contrast, a precise statement of the system's transfer behavior is made in the frequency domain.

A Digital Twin of the test bench can compensate for the deviation between a powertrain test bench setup and the related real vehicle characteristic (see chapter 3). A transfer function estimation is sufficient for low-frequency phenomena like handling or drivability, especially incorporating the effort for parameterization of a white-box Digital Twin modeling approach.

Compensation for the dead time is recommended to improve the test bed's controller performance further. Instead of using the scalar time delay information of the step response analysis in the time domain, we utilize the group delay information derived from the frequency domain. By conducting a Fast Fourier Transform (FFT) or estimation of the Frequency Response Function (FRF) with adequate estimators (e.g. based on the Welch method), a representative transfer function for the test bench control loop is determined [8].

Eq. 9 gives the phase $\arg\big(G(j\omega)\big)$ of the FRF, which consists of the system´s input function U and corresponding output function Y [10, p. 250]:

$$\arg\big(G(j\omega)\big) = \arg\big(Y(j\omega)\big) - \arg\big(U(j\omega)\big) \qquad \text{Eq. 9}$$

Based on the phase information, we calculate the group delay τ_{Gr} as the negative derivative of the same (Eq. 10) [11, p. 94]:

$$\tau_{Gr}(G(j\omega)) = -\frac{d}{d\omega}\arg\big(G(j\omega)\big) \qquad \text{Eq. 10}$$

Finally, the group delay provides information about the time delay of a signal in correspondence to its frequency. Therefore, for dynamic maneuvers at a racetrack, the group delay knowledge of a closed loop test bench operation enhances the frequency matching significantly.

The subsequent chapter presents the generation of a Digital Twin of a powertrain test bench. With a Digital Twin, the test bench characteristic is represented in both domains shown in chapter 2.

3 Generating a Digital Twin of a Powertrain Test Bench

A powertrain test bench can be used for several types of test cases. This paper focuses on one distinctive test scenario, racetrack testing. Therefore, the unit under test (UUT) should be operated in a manner that accurately replicates the dynamics witnessed during its usage by a professional race driver in a racetrack setting. The PTB has two different control modes to fulfil this scenario.

In the n/α-control mode previously logged wheel speed values (n) are used for speed control of the dynos. The logged values of the driving pedals (α) are used to control the powertrain under test. These values are either calculated in vehicle simulations or measured during test drives. However, this control mode has some disadvantages. As shown in chapter 2, the dynamics of car and test bench differ. Therefore, using logged wheel speed as a manipulated variable for the dyno control results in deviating loads at the UUT. Furthermore, the test would be executed with different UUTs. These can show deviant behavior to the UUT used for logging the control values, resulting in deviating loads. In summary, the test bench acts in a predetermined manner and does not respond to the UUT. [7]

The road load simulation (RLS) control eliminates this main disadvantage. Therefore, a model of the environment and residual vehicle calculates the resistance forces and the road tire contact. Utilizing the input variable (n_{Wheel}, Fig. 3) the simulation initially computes the slip. Subsequently, the tire model determines a transmissible torque at the tire based on the slip and the vehicle's tire contact forces. The inertia of the tire can either be assembled to the dynos or be simulated separately. Within this control mode, the manipulated variable of the dyno is calculated in a closed loop and dependent on the UUT. The control variable of the UUT can be obtained from logged values of the drive pedal, which still results in deviations if the UUT exhibits different behavior during logging. So, a model of a driver is implemented. The Driver calculates a deceleration and accelerator position from a predefined velocity trajectory and the simulated car velocity. These control modes are referred to as RLS/α or RLS/v. [7],[11]

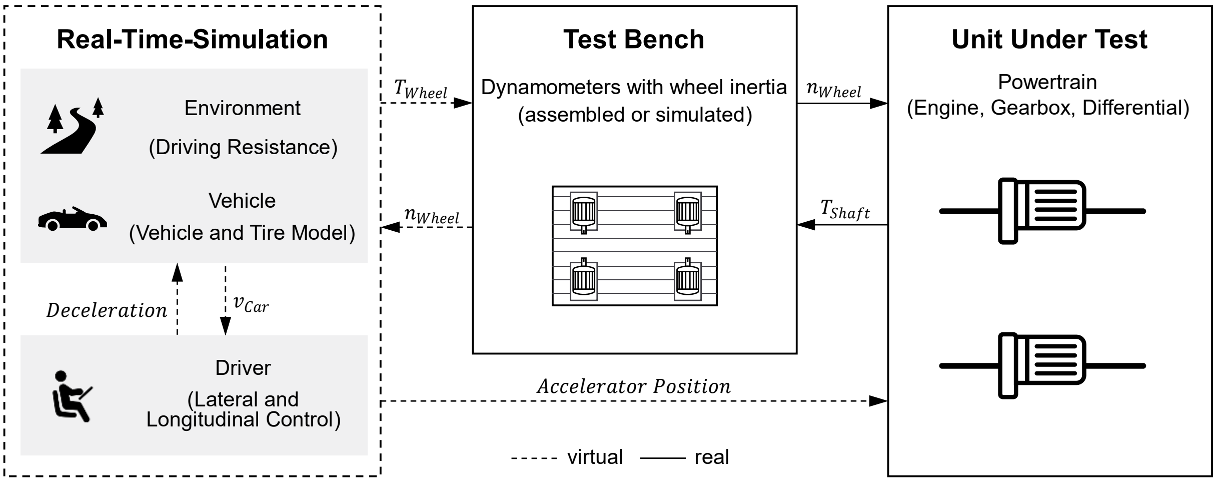

Fig. 3 Diagram of virtual and real components of a powertrain test bench [3]

Due to the listed advantages, RLS is the most suitable control mode to accurately reproducing tests on the racetrack. In addition, the driver model plays a crucial role in generating the accelerator pedal as an input signal for the UUT. To achieve realistic test results with this setup, it is essential to parameterize the simulation adequately. These parameters can be derived from simulations, measurements, or databases. However, due to data availability and model simplifications, there can be differences between the racetrack measurements and the tests conducted on the test bench.

Now one could use this test bench setup in combination with optimization algorithms to iterate a good setup of the simulation. However, applying optimization algorithms at a real powertrain test bench entails two primary disadvantages. Firstly, these algorithms require numerous iterations to converge and find a global solution to the optimization problem. At a test bench, it is not possible to parallelize the iterations, and they can only be executed in real-time. As a consequence, this approach demands considerable costs and time consumption. Secondly, using random parameter combinations by the algorithm poses a risk, especially when working with real components in the test bench setup. The selection of inappropriate parameter combinations could potentially cause damage to the UUT.

For the efficient application of optimization algorithms, the authors derived a Digital Twin of the powertrain test bench, as documented in [3]. The virtual Powertrain in the Loop test bench mirrors the structure of the physical test bench. It comprises three primary parts, as shown in Fig. 3. The real-time simulation is transferred to an offline system, necessitating parameterization of all interfaces with non-modeled systems. The Dynamometers and tire inertias are modeled based on the methods presented in chapter 2. Additionally, accurate replication of the UUT is essential. The models of the previous publication where data-based and physical models. Because data is often missing in the preliminary stages of the development process, the Digital Twin framework was expanded to include a physical powertrain library.

4 Optimization of Simulation Parameters by Comparing Measurement Data from Road Test and PTB using the Digital Twin

The optimization of the real-time simulation parameters should result in a more realistic behavior of the real-time simulation models by comparing road test measurement data and PTB measurement data. During tests on the powertrain test bench, mechanical loads on the powertrain are in focus. In RLS/v control, the modeling of the tire-road contact, as one part of the real-time simulation models, has a large influence on the resulting loads. The tire-road contact is mainly determined by the tire model and the tire contact forces. The tire model used on the PTB is sufficiently validated and is therefore not considered further. In the following, the modeling of the tire contact forces is examined in more detail to setup the optimization environment.

4.1 Sensitivity Analysis of Tire Contact Forces

The tire contact forces on all four tires are influenced by the following factors:

- **Weight force** (Vehicle mass m, gravity g and center of gravity x_{CoG})
- **Vehicle aerodynamics** (lift coefficients c_{Lift}, frontal area A, air density ρ_{Air} and vehicle speed v)
- **Longitudinal wheel load shift** (pitch due to longitudinal acceleration a_x, center of gravity height h_{CoG} and wheelbase l.
- **Lateral wheel load shift** (roll due to lateral acceleration a_y, rolling centre x_{RC} and track b)
- **Road course** (longitudinal and lateral inclination, excitation by the surface)

In this example, the excitation from the road surface is imported into the real-time model as a distance-based signal. In addition, longitudinal and lateral inclinations take only small values, so the influence of the road course is not considered further (cosine for small angles about one). The chassis affects the tire contact forces in the vehicle by damping the pitching and rolling due to longitudinal and lateral acceleration. Since the PTB's real-time models focus on real-time capability, the chassis is modeled rudimentary by a low-pass filter. Therefore, the tire contact forces are considered an optimization object. The following equations (Eq. 11-15) show the modeling of the tire contact forces in the real-time model:

$$Fz_{rear,left} = m\left(\frac{1}{2}\left(x_{CoG}\, g + a_x \frac{h_{CoG}}{l}\right) - (1 - x_{RC}) a_y \frac{h_{CoG}}{b_{rear}}\right) + F_{Lift,rear} \qquad \text{Eq. 11}$$

$$Fz_{rear,right} = m\left(\frac{1}{2}\left(x_{CoG}\, g + a_x \frac{h_{CoG}}{l}\right) + (1 - x_{RC}) a_y \frac{h_{CoG}}{b_{rear}}\right) + F_{Lift,rear} \qquad \text{Eq. 12}$$

$$Fz_{front,left} = m\left(\frac{1}{2}\left((1 - x_{CoG}) g - a_x \frac{h_{CoG}}{l}\right) - x_{RC} a_y \frac{h_{CoG}}{b_{front}}\right) + F_{Lift,front} \qquad \text{Eq. 13}$$

$$Fz_{front,right} = m\left(\frac{1}{2}\left((1 - x_{CoG}) g - a_x \frac{h_{CoG}}{l}\right) + x_{RC} a_y \frac{h_{CoG}}{b_{front}}\right) + F_{Lift,front} \qquad \text{Eq. 14}$$

$$F_{Lift,front/rear} = \frac{1}{4} c_{Lift,front/rear}\, A\, \rho_{Air}\, v^2 \qquad \text{Eq. 15}$$

The Digital Twin of the test bench is used for the comparison between vehicle measurement data and PTB measurement data, as the influence of individual parameters can be determined there with little effort. Theoretically, each parameter from the above formulas can be used as an adjustment variable to optimize the simulation quality of the Digital Twin, whereby a_x, a_y and v are to be understood as time-varying input variables. The selection of tunable variables, which only influence the input variables a_x, a_y and v independently, offers the advantage of a stepwise optimization.

4.2 Optimization Environment

To be able to compare the tire contact forces between the vehicle and Digital Twin, the high-frequency excitation of the road surface is filtered out of the vehicle measurement data using a low-pass filter since the excitation of the road surface is fed as a distance-based signal in the test bench respectively the Digital Twin.

To evaluate the quality of the results, a linear regression analysis is performed, comparing the vehicle measurement data with the simulation data obtained from the Digital Twin. Therefore, the analysis uses the slope m and the coefficient of determination R^2 of the regression line as quality measures. In an ideal scenario, when the vehicle and simulation measurement data align perfectly, the slope m equals 1, and the coefficient of determination R^2 reaches 100%.

Fig. 3 shows the optimization environment. A genetic algorithm is used as an optimizer [12]. Like most optimizers, the genetic algorithm minimizes a scalar, so an error measure e must be calculated from the quality measures m and R^2 (Eq. 16).

$$e = \frac{1 - R^2}{2} + \frac{|m - 1|}{2} \qquad \text{Eq. 16}$$

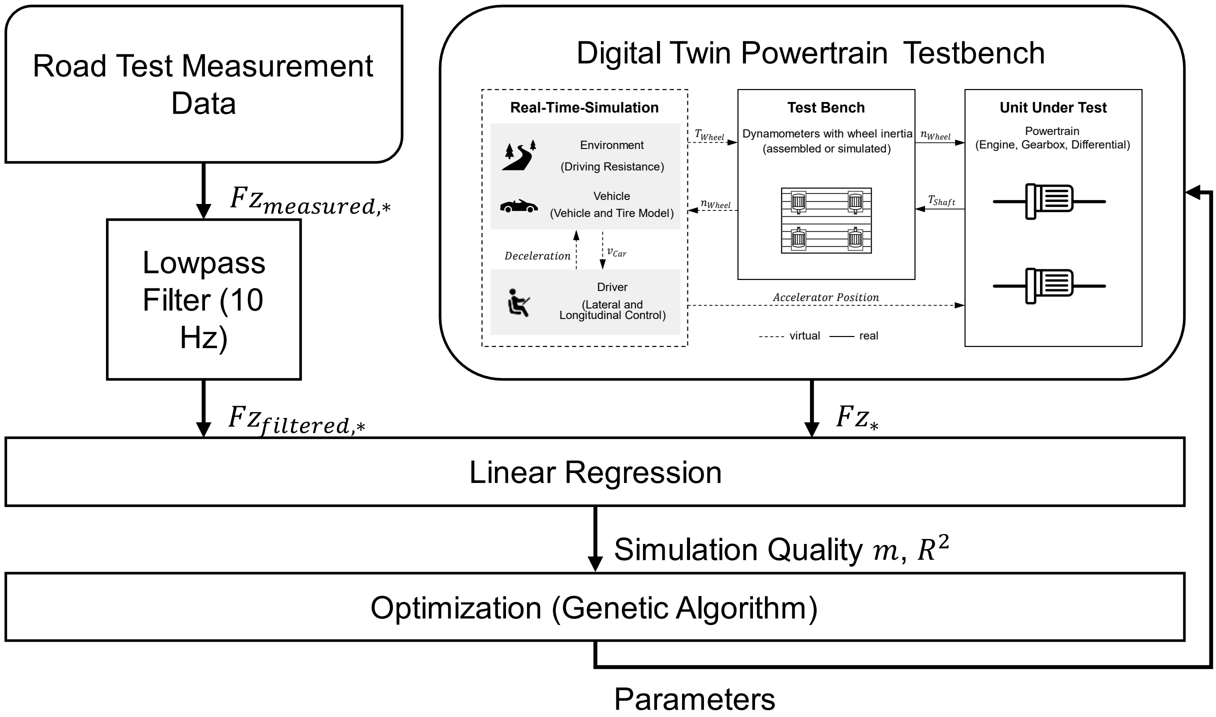

Fig. 4 Optimization environment in which low pass filtered vehicle measurement data is compared with simulation data from the Digital Twin to determine optimized parameters.

The RLS uses distance-based setpoint values (target speed and excitation by the road surface). The great advantage of this approach is that different powertrain setups (e.g. different power ratings) can be compared. Fig. 5 illustrates the advantage of this method. The reference speed was generated with a vehicle with more power and a better braking system than the later setup on the test bench. With a time-based reference, the speed deviations add up with time. This effect, therefore, also affects the calculation of the error values (Fig. 5 bottom). In the right part of the figure, the reference values are recorded on a distance basis, which means that the vehicle and test bench measurements are comparable despite the different powertrain setups.

Another application is testing fast laps on a racetrack with different powertrain setups. Two powertrains with different power ratings would set exactly the same lap time with a time-based reference speed. However, the more powerful powertrain will achieve a better lap time if the reference speed is based on distance.

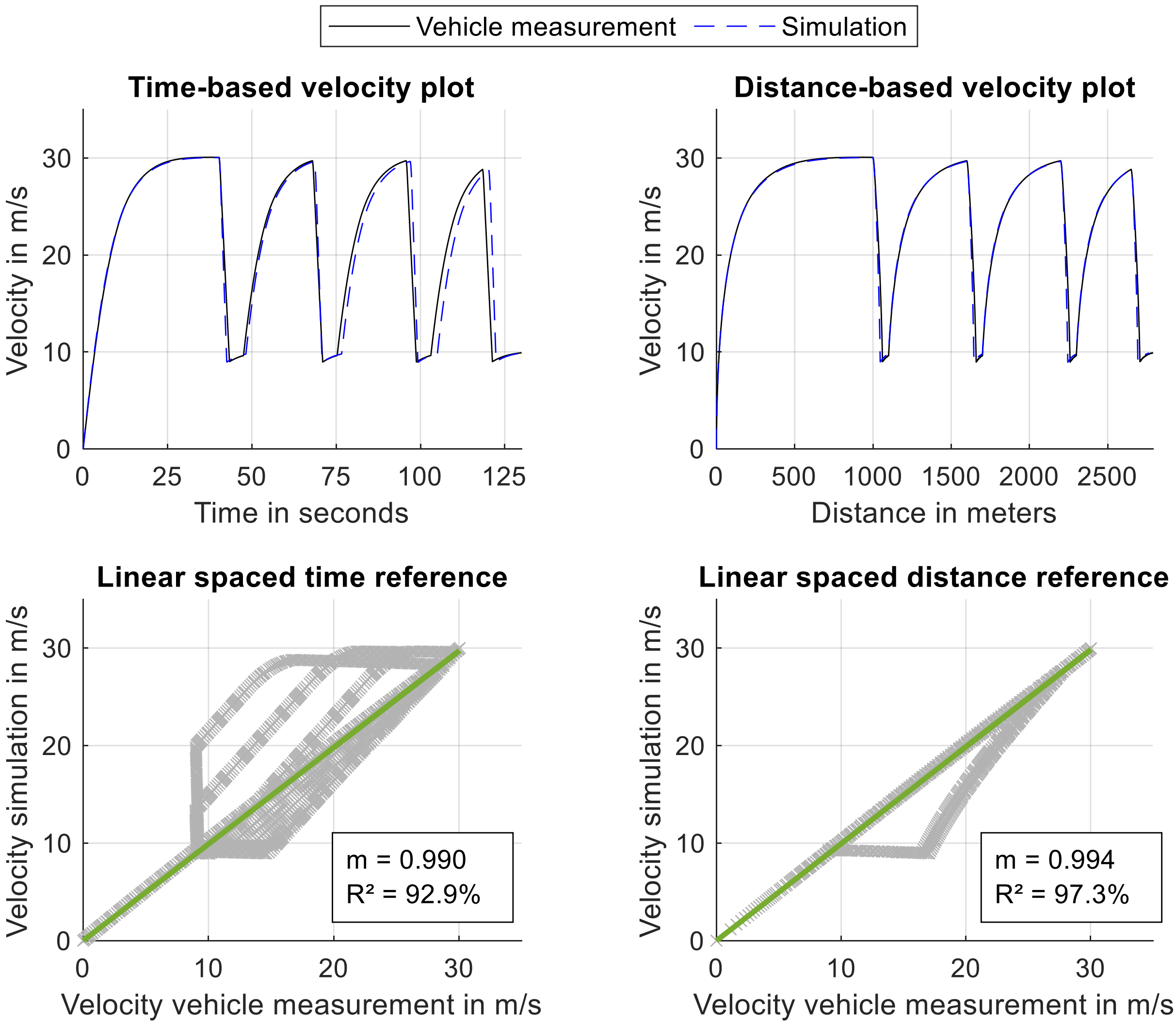

Fig. 5 Case study: Time- and distance-based data comparison

However, this method also has an influence on the optimization process. The data is recorded with a time-based sampling frequency. Calculating the error values of this data would result in a biased error calculation, as shown above. It is, therefore, necessary to compare the data on a distance basis. In order to calculate the referenced error values (R^2, m), linear spaced recorded data is also required.

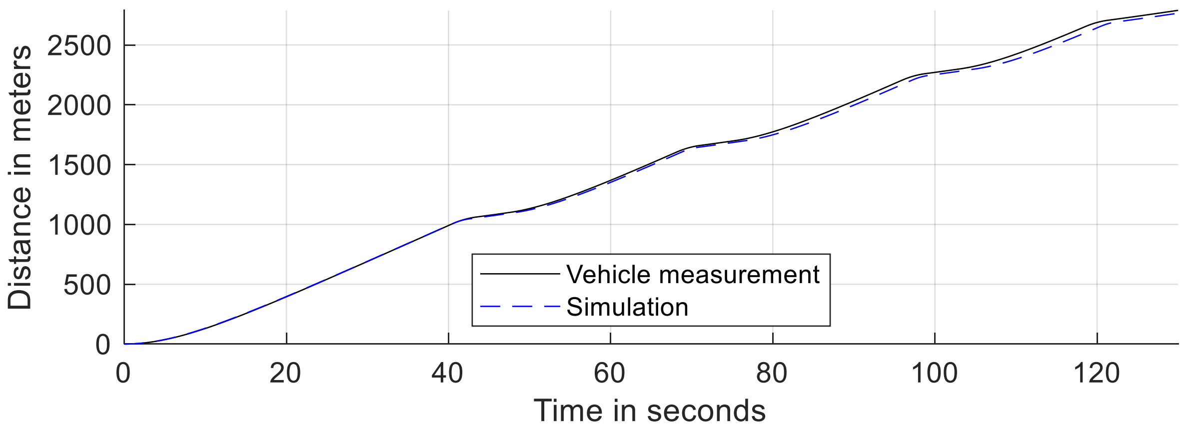

Fig. 6 Non-linearity between time and distance

Nevertheless, the non-linearity between time and distance can be seen in Fig. 6. Therefore, the first step in the optimization process is to create a linear-spaced distance vector from the distance data recorded at linear-spaced times. The second step is interpolating the recorded signals into the linear-spaced distance vector. The error values can then be calculated.

4.3 Optimization Procedure

As a primary step, it is recommended to compare the sum of the tire contact forces Fz_{sum}. Assuming vehicle mass and acceleration due to gravity to be correctly given values, the calculation of Fz_{sum} allows the consideration of the influence of vehicle aerodynamics (Eq. 17 and Eq. 18).

$$Fz_{sum} = Fz_{rear,left} + Fz_{rear,right} + Fz_{front,left} + Fz_{front,right} \qquad \text{Eq. 17}$$

$$Fz_{sum} = m\,g + \frac{1}{2}\left(c_{Lift,rear} + c_{Lift,front}\right) A\,\rho_{Air}\,v^2 \qquad \text{Eq. 18}$$

The comparison uncovered a parameterization error in the lift coefficients $c_{Lift,*}$ in the Digital Twin. The corrected values lead to a significant improvement regarding m, as shown in Tab. 1 (Step 1). In the next step, the tire contact forces are optimized by tuning wheelbase und both track widths of the simulated vehicle, because they influence the input variables a_x, a_y and v independently. The optimization improved the simulation quality, as shown in Tab. 1 (Step 2).

Tab. 1 Quality of the simulation data from the Digital Twin compared to the vehicle measurement before and after optimization in the three sub-steps and overall.

step	validation signal(s)	optimized parameters	error measure e	
			initial	optimized
1	Fz_{sum}	$c_{Lift,front}$: -50% $c_{Lift,rear}$: $-50\ \%$	$e\ =\ 0.158$	$e\ =0.121$
2	$Fz_{rear,left}$	b_{front}: $-27\ \%$ b_{rear}: $-12\ \%$ l: $+13\ \%$	$e\ =\ 0.118$	$e\ =\ 0.119$
	$Fz_{rear,right}$		$e\ =\ 0.124$	$e\ =\ 0.112$
	$Fz_{front,left}$		$e\ =\ 0.139$	$e\ =\ 0.119$
	$Fz_{front,right}$		$e\ =\ 0.158$	$e\ =\ 0.144$

4.4 Discussion

By far, the most significant contribution to enhancing simulation quality was the identification of parameterization errors related to the lift coefficients. Under normal circumstances, an improvement in simulation quality to this extent is, therefore, not to be expected. However, this case shows that the approach can also be used to check the plausibility of simulation results.

Virtual wheelbases are represented by the optimized wheelbase l and the optimized track widths b_{front} and b_{rear}, which depicts the influences of the chassis in the real car compared to the rudimentarily modeled chassis in the real-time simulation model.

In Fig. 7, the validation signal Fz_{sum} (filtered at the top, unfiltered at the bottom) is plotted over one lap of the racetrack. The filtered signal shows a 23% reduction in the error value. Especially in the first third of the lap, the presented method could reduce the deviation between vehicle measurement and simulation. The lower figure shows that an exact reproduction of the high-frequency oscillations is impossible with the current setup. A detailed track and chassis model would be required.

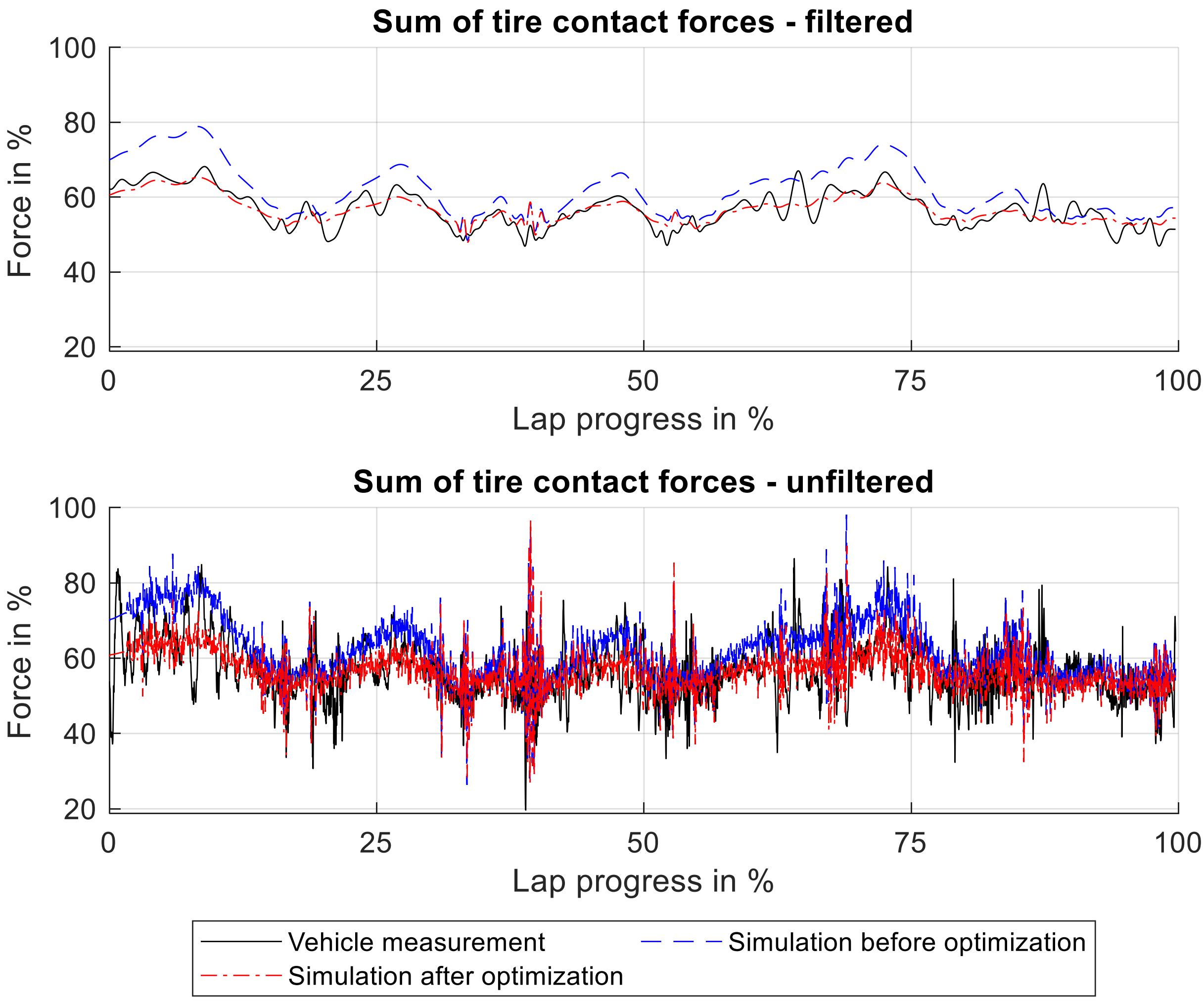

Fig. 7 Result of the optimization process for the vehicle model's sum of tire contact forces

This method has been performed by using the chassis model as an example. The approach can also be applied to other simulation parameters or models, such as unknown environmental parameters (friction coefficient tire-road).

5 Conclusion and Outlook

In the previous chapters of this research, a method for reducing the deviations between vehicle and test bench tests by adjusting the parameterization of real-time models in an optimization process was proposed. First of all, a detailed analysis of the test bench hardware was performed. This provides an insight into the mechanical and time-dynamic behavior. Subsequently, various modeling approaches in the form of transfer functions were explained with the behavior obtained. The derived information and modeling approaches were then combined with the Digital Twin of a test bench to create a safe and fast environment for optimization algorithms.

The following two-step optimization process started with a physical sensitivity analysis of model parameters. The lift coefficients were identified as sensitive parameters for the first step and optimized to the sum of the tire contact forces. The second step individually considered the tire contact forces and optimized the car's wheelbase and track width values. In a renewed comparison of the vehicle measurement with the simulation results of the Digital Twin using optimized parameters, improvements in the replication quality could be observed.

An important further step is the implementation of the updated parameters at the real test bench to achieve more realistic results in the upcoming tests. Furthermore, this method can be transferred to other real-time models, as the driver model.

6 Acknowledgement

The authors would like to thank Henri Siitonen for the initial setup of the project and for providing the measurement data and vehicle information.

7 Abbreviations

EDU	Electric Drive Unit
FFT	Fast Fourier Transform
FRF	Frequency Response Function
HIL	Hardware-in-the-Loop
HV	High voltage
RLS	Road-Load-Simulation
UUT	Unit Under Test

8 References

[1] Fuchs, Martina; Westermeyer, Johannes, 2023
Automobilindustrie [Automotive Industry]
In: Elmar Kulke (Ed.): Wirtschaftsgeographie Deutschlands.
Berlin, Heidelberg: Springer Berlin Heidelberg, pages 215–225.
ISBN: 978-3-662-65070-7

[2] Kochem, Michael; Kemper, Henning; Bilgic Istoc, Sami, 2023
Daten- und Workflowmanagement für die virtuelle Entwicklung softwaredefinierter Fahrzeuge [Data and Workflow Managament for the Virtual Development of Software-Defined Vehicles].
In: ATZ Automobiltech Z 125, pages 74–79.
DOI: 10.1007/s35148-023-1627-z

[3] Veith, Jan-Michael; Schilling, Jannes, 2022
Parametrierung und Optimierung eines Fahrreglers mittels virtuellem Antriebsstrangprüfstand [Paramterization and Optimization of a Drive Controller by a Virtual Powertrain Test Bed]
In: 9. AutoTest Fachkonferenz. Stuttgart 2022

[4] Dresig, Hans; Holzweißig, Franz, 2016.
Maschinendynamik [Machine dynamics]. 12th ed.
Heidelberg: Springer Berlin Heidelberg.
ISBN 978-3-662-52712-2

[5] Weber, S.; Dursun, Y.; Kirschbaum, F.; Jakobi, R.; Bäker, B.; Fischer, J., 2017.
Investigations of the process of road matching on powertrain test rigs.
In: 17. Internationales Stuttgarter Symposium. Stuttgart, 2017.
Wiesbaden: Springer Fachmedien Wiesbaden, pages 409-423.
DOI: 10.1007/978-3-658-16988-6_94

[6] Pfister, Felix; Fleck, Andreas, 2017.
Verfahren zum Steuern, insbesondere Regeln, eines Antriebsstrangprüfstands mit realem Getriebe [Method for controlling a powertrain test bench with real transmission].
Austrian patent AT 519553 B1, filed Apr. 07, 2017, and issued Aug. 15, 2018.

[7] Bauer, Robert, 2011.
Neues Regelkonzept für die dynamische Antriebsstrangprüfung [New control concept for dynamic powertrain testing]
In: 17. Steirisches Seminar über Regelungstechnik und Prozessautomatisierung, 2011
Institut für Regelungs- und Automatisierungstechnik, Technische Universität Graz
ISBN: 978-3-901439-09-4

[8] Schmidt, Henrik; Prokop, Günther, 2023
Experimental Analysis of Powertrain Test Bed Dynamometers for Black Box-Based Digital Twin Generation
In: 2023 IEEE Transportation Electrification Conference 2023. Detroit, MI, USA.
DOI: 10.1109/ITEC55900.2023.10187073

[9] Lunze, Jan, 2020
Regelungstechnik 1: Systemtheoretische Grundlagen, Analyse und Entwurf ein-schleifiger Regelungen [Control theory 1: Systems theory basics, analysis and design of single-loop control systems]. 12th ed.
Berlin: Springer Vieweg.
ISBN: 978-3-662-60746-6

[10] Meyer, Martin, 2021
Signalverarbeitung: Analoge und digitale Signale, Systeme und Filter [Signal Processing: Analog and digital signals, systems and filter]. 9th ed.
Wiesbaden: Springer Fachmedien Wiesbaden.
DOI: 10.1007/978-3-658-32801-6.

[11] Germann, Stefan; Nonn, Harald; Kopecky, Wolfgang; Abler, Georg; Witte, Lothar; Xuan, Hai Tran; Pfeiffer, Michael; Brodbeck, Peter
Verfahren zum Simulieren des Verhaltens eines Fahrzeugs auf einer Fahrbahn [Method for Simulation of the Behavior of a Vehicle at a Road]
European Patent: EP 1037030 B1, filed Mar. 12, 1999, issued Sep. 20, 2000

[12] Conn, Andrew; Gould, Nicholas; Toint, Philippe, 1997
A globally convergent Lagrangian barrier algorithm for optimization with general inequality constraints and simple bounds
In: Math. Comp. 66 (217), S. 261–289.
DOI: 10.1090/S0025-5718-97-00777-1.

Imprint

Publisher

Institute for Automotive Engineering (ika), RWTH Aachen University
Univ.-Prof. Dr.-Ing. Lutz Eckstein
Steinbachstraße 7, 52074 Aachen
Phone: +49 241 80-25600
Fax: +49 241 80-22147
E-Mail: office@ika.rwth-aachen.de

Chair of Thermodynamics of Mobile Energy Conversion Systems (TME), RWTH Aachen University
Univ.-Prof. Dr.-Ing. Stefan Pischinger
Forckenbeckstraße 4, 52074 Aachen
Telefon: +49 241 80-48000
Telefax: +49 241 80-22995
E-Mail: office@tme.rwth-aachen.de

Distribution

Aachener Kolloquium Fahrzeug- und Motorentechnik GbR
Steinbachstraße 7, 52074 Aachen
Phone: +49 241 88-61251
Fax: +49 241 88-61266
E-Mail: info@aachen-colloquium.com

1st Edition October 2023

www.aachen-colloquium.com

ISBN 978-3-00-076758-6